International Journal of Energy Research

WILEY

RESEARCH ARTICLE OPEN ACCESS

Assessment of Combined Wave and Wind Energy Resources of the Marine Pastures in Shandong Peninsula

Yong Wan | Qiuwei Cheng | Xiaoshun Feng | Yongshou Dai

College of Oceanography and Space Informatics, China University of Petroleum, Qingdao 266580, China

Correspondence: Yong Wan (wanyong@upc.edu.cn)

Received: 15 August 2024 | **Revised:** 7 September 2025 | **Accepted:** 25 September 2025

Academic Editor: Paul Adedeji

Keywords: applicability assessment | combined wave and wind energy | ERA5 reanalysis | wave energy | wave energy converter | wind energy | wind turbines

ABSTRACT

The rapid development of the Blue Economic Zone on the Shandong Peninsula has generated a huge demand for renewable energy. Sensibly developing and utilizing these resources can provide a stable energy supply for marine pastures. However, assessing energy development potential must be done before the resources are developed. Using the fifth-generation atmosphere reanalysis dataset (ERA5) from the European Centre for Medium-Range Weather Forecasts (ECMWF) over nearly 15 years, this study assessed the combined wave and wind energy potential around the Shandong Peninsula's marine pastures. A method was proposed to determine sites for combined wave and wind energy, analyzing the abundance, availability, stability, and correlation (CO) of these two resources in the sea surrounding the marine pastures. This novel approach addresses the limitations of traditional, disparate evaluation systems for wave and wind resources, enhancing assessment efficiency and accuracy. Utilizing the Joint Zoning Coefficients (JZCs) derived from these four indexes and considering the constraints related to the distance from the marine pastures, the VIOKR methodology was used to identify the four key sites most suitable for resource development. The JZC innovatively incorporates indicator weights and optimal station construction distance, a feature often overlooked in previous multi-indicator assessments, to provide a more scientific basis for site selection. At these sites, the propagation direction as well as the cross-CO with different time lags were analyzed. Finally, the most suitable wave energy converters (WECs) and wind turbines (WTs) have been identified, and the distribution of power generation times for different device combinations has been analyzed. This comprehensive device selection and power generation analysis aims to maximize energy conversion efficiency and ensure stable power output for marine pastures. The study findings offer decision-making support for the combined wave and wind energy resources in the Shandong Peninsula.

1 | Introduction

At present, there is a noticeable acceleration in the global transition from a high-carbon energy system predominantly based on fossil fuels to a low-carbon energy system dominated by renewable energy sources [1]. In 2020, renewable energy sources were projected to provide around 13% of the world's total energy consumption. In addition, there are currently new research advances on mitigating climate change, emphasizing the importance of achieving renewable energy transitions [2]. High initial construction and maintenance costs have slowed the technological development of renewable energy sources such as wave and wind power. This challenge underscores the heavy reliance on tractable numerical models for the conception and optimization of energy converters, which necessitates a delicate balance between accuracy and computational costs [3]. In addition, submarine cables are expensive, raising electricity transportation. In addition to cost challenges, the intermittency and instability of renewable energy generation must also be addressed [4]. Therefore, simultaneous extraction of multiple ocean energy sources within the same marine area could reduce the uncertainty when relying on a single source of energy [5].

Combining wave and wind energy resources in the same region can significantly enhance spatial utilization and energy conversion efficiency. Nezhad et al. [6] identified the optimal areas for installing wind turbines (WTs) in the Mediterranean basin and effectively predicted wind speeds in the region using LSTM. Gonzalo et al. [7] developed an integrated assessment model (IAM) and introduced a new method that can be used to model the variability of renewable energy on an hourly basis. However, before resource development, it is essential to assess the energy development potential in the study area and determine the most suitable sites for resource exploitation. Resource development, particularly for complex systems like combined wave and wind energy, often involves multiple, conflicting criteria. Multi-criteria decision analysis (MCDA) techniques have emerged as powerful tools to evaluate and select optimal sites or solutions by systematically considering various influential factors. MCDA is a formal and structured decision-making methodology that can be used for comparing different alternatives and exploring decisions in the case of situations with multiple and conflicting criteria [8]. These methods allow for a structured approach to decision-making, moving beyond simple single-factor analyses to incorporate diverse considerations such as resource abundance, stability, availability, and economic viability. The application of MCDA is widespread, with various models being employed to solve complex decision-making problems across different fields, such as waste management [9]. As energy management problems are getting more complex, economic considerations are complemented with environmental and social considerations, leading to multiple-criteria decision-making being used to deal with conflicting decision problems [10]. For instance, in the context of renewable energy, geographic information system (GIS) interfaces are often combined with MCDA to visualize and analyze geospatial data, allowing for the evaluation of multiple, usually overlapping, criteria to determine optimal sites [11]. This GIS-MCDA-based approach has been identified as a highly effective method for the spatial siting of offshore wind farms and other marine energy projects [12]. For example, common methods include the analytic hierarchy process (AHP), the full consistency method (FUCOM), and the ViseKriterijumska Optimizacija I Kompromisno Resenje (VIKOR). AHP is computationally simple and can address intuitive problems, but it can become complex when dealing with multi-decision problems [13]. FUCOM is known for its strong objectivity, fewer pairwise comparisons, and higher consistency in weight determination, making indicator weight allocation more reliable and less subjective. VIKOR excels at handling multi-criteria conflicts and providing compromise solutions, offering a strong alternative to AHP. Compared to other research conducted worldwide, there has been more focus on studying individual resources, with only a limited number of studies examining the feasibility of combining wave and wind energy resources. Current approaches to assessing wave and wind energy resources often employ two independent evaluation systems, which can lead to inefficient assessments. Furthermore, traditional methods frequently assume equal importance for various indicator elements or simply sum/multiply them, thereby overlooking the dynamic influence of changes in sea area locations on indicator weights. This oversight can result in assessment deviations and fail to accurately reflect the true contribution of each indicator in different regions. In 2017, Kalogeri et al. [4] analyzed the suitability of locations in European offshore areas for resource co-development, considering aspects like availability, variability, consistency, correlation (CO), and extreme values. In 2018, Rusu et al. [14] conducted a comprehensive evaluation of both wave and wind energy in the Black Sea basin, utilizing a 20-year dataset. They analyzed seasonal variations, variation coefficients, skewness, and kurtosis to identify potential areas for the combined development of these resources. In 2019, Azzellino et al. [15] explored the possibility of wave and wind energy resource co-development in Australian waters from a CO perspective. They also used spatial planning methods to identify suitable locations for both resource types. In 2020, Ferrari et al. [16] developed an availability index based on the CO and abundance of wave and wind energy resources. Their study identified the specific areas within the Mediterranean Basin that are best suitable for combined development. In 2021, Lira-Loarca et al. [17] assessed the optimal time availability of combined wind and wave resources in the context of climate change using the ES index. In 2022, Gao et al. [18] analyzed multiple locations around the Australian coastline for offshore wind and wave energy. Their study evaluated energy availability, electricity fluctuations, consistency, CO, as well as annual and seasonal variations over a 7-year period to identify the optimal locations for development. In 2023, Rusu [19] conducted evaluations of wave and wind energy resources in the vicinity of the Iberian Peninsula, covering two distinct time frames: the past 20 years and the upcoming 20 years. In 2024, Gormüs et al. [20] conducted an assessment of the joint wind and wave resources in the Mediterranean and Black Seas by examining their development potential, directionality, CO, and complementarity.

Shandong Province's Blue Economy Zone is the pioneering regional development strategy centered on the marine economy in China. Accelerating resource development in the Shandong Peninsula is an inevitable choice to implement the strategic deployment of "Carbon Peak" and "Carbon Neutral." Currently, research on resource assessment in the Shandong Peninsula has been limited to individual resources. Huiqun and Qifeng [21] examined the distribution of wind energy resources in Shandong Province. Their results indicate that the coastal areas of Shandong Province boast rich wind energy resources, with a wind power density of around 320 W/m^2, especially in the northern coastal regions. Wan and Liu et al. [22, 23] assessed the potential for wave energy resources. Their results indicate that Shandong's coastal areas have comparatively lower wave energy resources with a wave power density of around 2 kW/m. The areas with more abundant resources are primarily found in the eastern and southeastern nearshore regions, particularly in the vicinity of Rongcheng. The wave and wind energy resources in the Shandong Peninsula are relatively low to medium. In this context, the synergistic use of wave and wind energy resources is more favorable than developing them independently, as previously discussed. Prior studies have offered significant insights for the comprehensive evaluation of combined wave and wind energy resources.

However, as a new sustainable production mode of marine fisheries, while marine pastures are instrumental in the transformation and upgrading of China's marine fisheries, there has been a limited amount of research on combining marine pastures application scenarios with wave and wind energy resources, and there are no precedents in China for the pilot construction of wave and wind power sites around marine pastures. Marine pastures face the issue of insufficient offshore power resources, which prevents large-scale modern marine pasture operational equipment and monitoring facilities from being used stably and efficiently over the long term. Therefore, there is an urgent need to study a scientific site selection method for establishing combined wave and wind energy resources in marine pastures. First, in the preliminary analysis of wave and wind energy resource abundance, different units of evaluation metrics were employed, which reduced the comparability of the assessment results. This not only resulted in poor comparability of the evaluation results but also increased the complexity of integrating the two resources in practical applications. Therefore, this study first standardized the measurement units, enabling the scientific quantification of the abundance of wave and wind energy resources, thereby providing a solid foundation for subsequent resource integration analysis. In addition, in previous multi-indicator assessment work, the degree of importance of each indicator was not considered, and the distance between sites in different regions was ignored. Therefore, This article establishes a Joint Zoning Coefficient (JZC) based on multi-indicators. Innovatively, the concept of indicator weights was introduced, taking into account the importance of each indicator in the joint development. Additionally, this article is the first to introduce the key factor of optimal station construction distance, ensuring that wave and wind energy resources are effectively integrated in physical space, further optimizing the station layout.

Through this innovative site selection method, this article not only addresses the challenges in joint resource evaluation but also proposes a comprehensive and efficient site selection model, providing scientific guidance for the combined development of wave and wind energy in marine pastures. The contributions of this method are as follows: (1) By integrating wave and wind energy resources into the application scenarios of marine pastures, it fills a gap in this field in China, offering pioneering exploration for the sustainable energy development of marine pastures. Moreover, the optimal station construction distance was included in the site selection analysis for the joint development of wave and wind energy. (2) Addressing the issue of different evaluation metrics used in previous studies for wave and wind energy resource assessments, this research unified the measurement units and scientifically quantified the abundance of both resources, improving the comparability and accuracy of the evaluation results. (3) We expanded the range of indicators considered, making the evaluation more comprehensive. Based on these indicators, we constructed the JZC, which enhanced the precision of the evaluation. This comprehensive approach ensures a more accurate assessment. The remaining sections are structured as follows: in Section 2, the data and research methods for both energy sources are presented. In Section 3, the combined wave and wind energy resources are analyzed from four perspectives: resource abundance, availability, stability, and CO. The JZC is developed based on the FUCOM methodology within the optimal distance around the marine pastures. The most suitable sites are identified based on the VIKOR method. In addition, the performance of hybrid power stations combining different configurations of wave energy converters (WECs) and WTs was investigated at these sites, considering the direction of resource directionality and time-lag COs. Finally, in Section 4, this article provides an overview of the main findings.

2 | Materials and Methods

2.1 | Materials

2.1.1 | Study Area

The Shandong Peninsula is situated along the eastern coastal region of China. The marine area is about 159,600 square kilometers, with a total coastline length of about 3000 km. Coastal waters cover around 37% of this area. Shandong Province has abundant marine pastures, which can not only protect marine resources but also realize the recovery of fishery resources and "blue carbon sinks." This article selects the national-level marine pasture in the Shandong Peninsula with latitude and longitude ranging from 34.5°N–39°N to 118°E–125°E as the research area (Figure 1).

According to the website of the Ministry of Agriculture and Rural Affairs of the People's Republic of China and the resource abundance situation, a comprehensive list of national-level marine pasture demonstration areas has been compiled for Shandong Province. This list encompasses the eighth (2023), seventh (2022), and sixth (2020) batches in Shandong Province. A total of 14 national-level marine pastures are depicted in Figure 2, with the name of each marine pasture provided in Table 1.

If too close to the offshore power farm may cause noise impact and visual interference; if too far away, it will increase the maintenance cost and installation cost, so it is necessary to specify the minimum distance and the maximum distance that need to be maintained. Therefore, it is necessary to specify minimum and maximum distances. Thus, a potential development area suitable for the installation of the device is identified. The distance to the power farm should exceed 10 km according to the policy of the Chinese government, and considering the cost-effectiveness, the development of offshore energy sources should be set at a maximum distance of 30 km from the coast [24]. Therefore, this article adopts these criteria to define the study area, ranging from 10 to 30 km from the marine pastures, as the potential development area.

2.1.2 | Study Data

Assessing wave and wind energy requires fundamental parameters, such as significant wave height (Hs, m), energy period (Te, s), and wind speed (V, m/s) In this study, all wave and wind data were sourced from ERA-5 data provided by the European Centre for Medium-Range Weather Forecasts (ECMWF). The ECMWF data have been utilized in numerous assessments of wind and wave resources, being recognized as the most dependable data source. Specifically, ERA5 data spanning 15 years from 1 January 2008 to 31 December 2022 were selected, featuring a spatial resolution of $0.125° \times 0.125°$ and a time interval of 6 h.

The accuracy of the parameters is paramount for the assessment work. This article uses a buoy in the study area (Buoy 001, location: 38.1585°N, 121.0680°E), which was deployed by the State Oceanic Administration of China in the nearshore area of the Shandong Peninsula during the Ocean Renewable Energy Special Fund Project (GHME), and most coastal waters in China are shallow. Wan et al. [25] compared the measured the data from the buoy with the

FIGURE 1 | The research area.

significant wave height (Hs) and energy period (Te) data provided by ERA5, confirmed the accuracy of the ERA5 data. Meanwhile, Shi et al. [26] also validated the accuracy of ERA5 wave field data using the Y1 buoy located at a depth of 13 m off the coast of the Shandong Peninsula. The aforementioned studies collectively demonstrate that the ERA5 data had enough accuracy to be used as the base data for follow-up research.

To validate the accuracy of the wind speed data provided by ERA5, Wan et al. [27] use the wind speed with buoy 006 deployed by the China National Marine Bureau during the Ocean Renewable Energy Special Project in the South China Sea. The research findings indicate that the root mean square error (RMSE) for significant wave height (Hs) compared to buoy 001 is 1.79 s, with a CC of 0.80. Additionally, Wang et al. [28] also confirmed the accuracy of ERA5

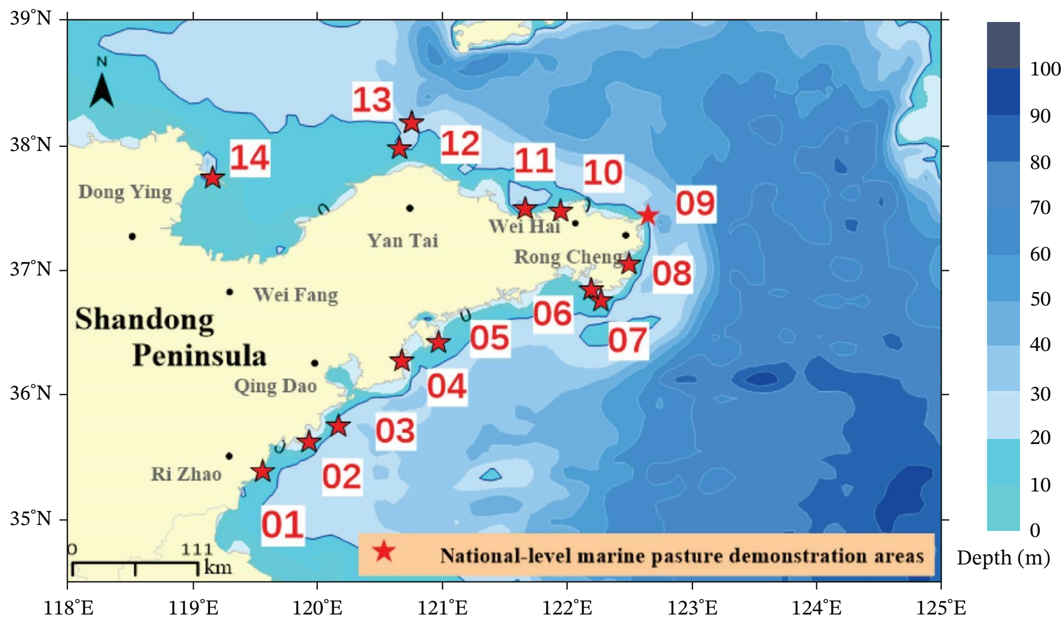

FIGURE 2 | Locations of marine pastures.

TABLE 1 | National-level marine pastures names.

Number	Name
01	Shenglong North Sea area of Rizhao Halong Bay
02	Ruizi the Sea area of Qingdao Zhaitang Island
03	Taoshengyijiu the sea area of Qingdao Lingshan Bay
04	Yiyida the sea area of Qingdao Laoshan Bay
05	Guoxin Southeast sea area of Qingdao Tianhengdao Island
06	Xinhong the sea area of Rocheng Jinghai Bay
07	Taoyuan the sea area of Rongcheng Sushan Island
08	Dongxing the sea area of Rocheng Boge Island
09	The sea area of Rocheng Chudao Island
10	Yutai the sea area of Weihai ShuangdaoBay
11	Kongji eastern sea area of Yantai Yangma Island
12	Zhongping the sea area of Changdao Xiaoheishan Island
13	Runfengyuan the sea area of Yantai Tuojidao Bay
14	Kanghua the sea area of Dongying Hekou District

wind speed. These studies collectively demonstrate that ERA5 wind speed data had enough accuracy to be used as the base data for follow-up research.

2.2 | Methods

2.2.1 | Method of Unified Metric Construction and Key Site Selection

To identify suitable areas, it is necessary to rely on appropriate evaluation indicators. Therefore, four evaluation indicators were constructed: the potential installed capacity (IC), the stability (ST) index), the availability ratio (AR), and the CO. Each indicator is designed to reflect the combined distribution of wave and wind energy. In constructing the potential IC index, the units of assessment were first harmonized to make the data more comparable. However, the assessment process is complicated and inefficient when using multiple indicators across different regions, and it leads to the unequal importance of these parameters. The allocation of weights needs to be refined and specified, so a JZC (Equation (1)) is established based on the importance of each indicator. This improves the flexibility and applicability by determining the importance of each indicator under different regions. It will determine the most suitable marine pastures for the development of both resources.

$$\mathrm{JZC} = a \times \mathrm{IC} + b \times \mathrm{ST} + c \times \mathrm{AR} + d \times \mathrm{CO}, \tag{1}$$

where a, b, c, and d represent the weight coefficients for each index. For the different characteristics of marine resources across different marine pasture scenarios, this study assigns different weighting factors to each of the four parameters for different marine pastures scenarios. The calculation process of the JZC is achieved by performing a weighted sum of four key indicators: IC, ST, AR, and CO. First, the FUCOM method is used to calculate the weights of each indicator, ensuring the rationality and consistency of the weight distribution. FUCOM is a weighted method based on linear programing, and compared to traditional methods, it has the advantages of reducing the number of comparisons and eliminating redundancy, making the weight calculation more efficient and accurate. Next, the scores of marine pastures for these four indicators are multiplied by their respective weights and summed to obtain the comprehensive evaluation—JZC. Through the precise weighting advantage of FUCOM, the JZC provides a more scientific basis for evaluating marine pastures development potential, optimizing resource allocation decisions. The detailed calculation methods for the weighting factors are provided in Appendix A [29]. Not only do we identify them, but we also need to select key sites for WECs and WTs deployment. To rank the development potential of various sites within a region and identify the site with the highest potential as the final installation location, VIKOR can effectively address the multi-criteria conflict present in the four indicators. By calculating the distance between each option and both the ideal and anti-ideal solutions, VIKOR finds a compromise solution that ensures the selected region achieves a more balanced performance across these four dimensions. This ultimately results in a comprehensive ranking of the development potential of each site in the critical development areas, providing decision-makers with more scientific and practical recommendations [30]. The detailed calculation are methods provided in Appendix B. In this study, we can comprehensively consider the factors of the four indicators as well as their relationships to make decisions. Compared to other algorithms, this method is better at balancing multi-objective conflicts, focusing on compromise solutions that aim to find a relatively balanced option across all criteria. It excels in multi-objective decision-making and evaluation scenarios by prioritizing a more even performance across conflicting goals. The specific calculation processes for the four indicators are as follows:

- The potential IC

The potential IC is a combination of potential IC of wave (IC_{wa}) and potential IC of wind (IC_{wi}). The advantage of using the potential installed capacities of the two types of energy in this study is that it standardizes the unit of measurement to kilowatts (kW) when assessing the abundance of both resources, instead of using different units such as wave energy flux (P_{wa}, kW/m) and wind power density (P_{wi} W/m^2). By establishing this indicator, wave and wind energy can be assessed using the same index. It is finally defined to be calculated as follows:

$$\mathrm{IC} = \mathrm{IC}_{wa} + \mathrm{IC}_{wi}. \tag{2}$$

Following the approach introduced by Wan et al. [31] to unify unit, the formula of IC_{wa} is as follows:

$$\mathrm{IC}_{wa} = P_{wa} \times \mathrm{Lon}_{len} \times \left(\frac{\mathrm{Lat}_{len}}{\lambda}\right), \tag{3}$$

$$\lambda = \frac{gT_e^2}{2\pi}. \tag{4}$$

where Lon_{len} is the longitudinal extent within the confined area, Lat_{len} is the latitude extent within the confined area (considering the latitude's influence), and λ is the wavelength, which can be computed based on the wave period (T_e). P_{wa} is the annual average wave energy flux, which is a critical parameter for assessing the exploitable potential. Because the coastal waters of the Shandong Peninsula are relatively shallow and the seabed terrain is complex, it is necessary to consider the nearshore effects when calculating wave energy flux, including the coastline or adjacent islands shielding, bottom dissipation, and so on. Therefore, this article uses the approach suggested by Wan et al. [31], which is suitable for calculating wave energy flux across different water depths to improve the accuracy of the wave power density. The following formula calculates as follows:

$$P_{\mathrm{wa}} = \overline{E}\left[\frac{gT_{\mathrm{e}}}{2\pi}\tanh(kd)\right]P_{\times}, \tag{5}$$

where $\overline{E} = \overline{1}/16\rho g H_s^2$ denotes the wave energy density (J/m^2), g denotes the gravitational acceleration (9.8 m/s^2), $k = \frac{2\pi}{\lambda}$ (m^{-1}), d is water depth (m), and $P_* = \frac{1}{2}(1 + \frac{2kd}{\sinh 2kd})$. Details of the calculations are given in the literature.

The formula of $\mathrm{IC_{wi}}$ is as follows:

$$\mathrm{IC_{wi}} = P_{\mathrm{wi}} \times \mathrm{Lon_{len}} \times \mathrm{Lat_{len}}. \tag{6}$$

P_{wi} is the average wind density power.

$$P_{\mathrm{wi}} = \frac{1}{2}\rho V^3, \tag{7}$$

where ρ denotes the density of air at standard atmospheric pressure (1.225 kg/m^3), V denotes the wind speed.

- Stability (ST) index

Research has indicated that resource stability is a crucial factor influencing power plant construction, and a stable resource is more suitable for energy development. The ST index is expressed as follows:

$$\mathrm{ST} = \frac{\sqrt{\frac{1}{N}\sum_{i=1}^{N}\left(P_{\mathrm{wa}} - \overline{P_{\mathrm{wa}}}\right)}}{\overline{P_{\mathrm{wa}}}} + \frac{\sqrt{\frac{1}{N}\sum_{i=1}^{N}\left(P_{\mathrm{wi}} - \overline{P_{\mathrm{wi}}}\right)}}{\overline{P_{\mathrm{wi}}}}, \tag{8}$$

where N denotes the total number of samples, $P_{\mathrm{wa}}, P_{\mathrm{wi}}$ denote wave energy flux and wind power density, and $\overline{P_{\mathrm{wa}}}, \overline{P_{\mathrm{wi}}}$ denotes the mean value. A smaller value for this change indicator signifies a more stable resource, making it more favorable for resource collection.

- AR

According to previous studies, for wind energy, the wind power density of 50 W/m^2 is considered the minimum benchmark for evaluating the abundance of wind energy resources. For wave energy, the wave energy flux greater than 2 kW/m is considered the minimum benchmark for evaluating the abundance of wave energy resources. Hence, this article utilizes the two criteria as minimum standards and evaluates them by the ratio of the available time of resources to the total time the available time of resources within a year. The AR is expressed as follows:

$$\mathrm{AR} = \frac{\text{Number of hours } P_{\mathrm{wa}} > \frac{2\mathrm{kW}}{m} \text{ and } P_{\mathrm{wi}} > \frac{50\mathrm{W}}{m^2}}{\text{Total number of hours} \times 100\%}. \tag{9}$$

- CO

If renewable energy sources can complement each other, the power generated will be smoother, thus reducing the problem of unstable energy supply caused by fluctuations in a single energy source [32]. The CO between the two can be expressed by the following expression:

$$c(\tau) = \frac{1}{N}\sum_{k=1}^{N-\tau}\frac{\left[P_{\mathrm{wa}}(k) - \overline{P_{\mathrm{wa}}}\right]\left[P_{\mathrm{wi}}(k+\tau) - \overline{P_{\mathrm{wi}}}\right]}{\sigma_{\mathrm{wa}}\sigma_{\mathrm{wi}}}. \tag{10}$$

$c(\tau)$ indicates the time delay between the two resources. c (0) denotes the same moment in time, which is important for uniform power output to the power output and reduced generation interruptions. Where $\sigma_{\mathrm{wa}},\sigma_{\mathrm{wi}}$ denote standard deviation values of the wave energy flux and wind power density.

2.2.2 | Determination Method of the Best Devices

After identifying the key sites most suitable for development, it is essential to determine the type of devices to be deployed. Many coastal cities in China have taken the marine pastures industry as a strategic emerging marine industry. It is known that Yangjiang City in the western region of Guangdong Province poised to initiate the construction of a marine pastures. The project site is located in Yangxi County, Shaguo Town, south of the sea. At present, the project has carried out the environmental impact assessment document review publicity. In this case, the vessel "Penghu" has a capacity of 10,000 m^3 of cultured water, and it is estimated that a marine pasture requires about 42 MW/year [33]. Based on the average output power and capacity factor, the most suitable WECs and WTs are selected for each site. The average output power is correlated with the rated power of the device, as well as the power matrix of the WEC and the power curve of the WT. The capacity factor represents the ratio of the average output power to the rated power, reflecting the actual conversion efficiency of both devices. The calculation methods are as follows:

$$P_{e\_\mathrm{wa}} = \frac{1}{100}\cdot\sum_{i=1}^{n_T}\sum_{j=1}^{n_H}P_{ij}\times f_{ij}, \tag{11}$$

$$P_{e\_\mathrm{wi}} = \frac{1}{100}\cdot\int_{\text{Cut-in speed}}^{\text{Cut-off speed}} f(t)p(t)dt, \tag{12}$$

$$C_{f\_\mathrm{wa}} = \frac{P_{e\_\mathrm{wa}}}{\text{Rated power}}\times 100, \tag{13}$$

$$C_{f\_\mathrm{wi}} = \frac{\exp\left(-\left(\frac{v_m}{c}\right)^k\right) - \exp\left(-\left(\frac{v_r}{c}\right)^k\right)}{\left(\frac{v_r}{c}\right)^k - \left(\frac{v_m}{c}\right)^k} - \exp\left(-\left(\frac{v_{\mathrm{off}}}{c}\right)^k\right), \tag{14}$$

where $P_{e\_\mathrm{wa}}, P_{e\_\mathrm{wi}}$ represents the average output power, P_{ij} represent the power output of the WECs, whose value for wave energy depends on the specific power matrix of the WECs, as calculated in [34]. f_{ij} represents the frequency of the two energies under different sea states. For WTs, $f(t)$ is the Weibull probability density function, $p(t)$ is the power curve, as calculated in [35]. C_{f_wa} represents the capacity factor of wave. C_{f_wi} represents the capacity factor of wind; where v_r, v_m, v_{off} are rated, cut-in, and cut-off speeds of the WTs, respectively. In article, three WECs devices

TABLE 2 | Individual parameters of the WECs and WTs.

Devices	SIEMENS	VESTAS	ENVISION
WTs			
Rated power (kW)	7000	8000	4200
Cut-in speed (m/s)	3	4	3
Rated speed (m/s)	13	13	12
Cut-off speed (m/s)	25	25	25
Rotor swept area (m^2)	18600	21164	13273
	Wave Star	**Oyster**	**CETO**
WECs			
Rated power (kW)	600	800	260
Suited water depth (m)	10–30	15	20–50

are chosen: Wave Star, Oyster, and CETO, three WTs are chosen: SIEMENS (SWT-7.0-154), VESTAS (V164 8 MW), and ENVISION (EN130-4.2). The main parameters are shown in Table 2.

3 | Results

3.1 | Combined Wind and Wave Resource Characterization and Key Site Selection

In order to analyze the distribution of combined resources for the four indicators, this study utilizes the indexes from Section 2.2.1, and the resulting graph is shown in Figure 3. As illustrated in Figure 3a, the total power index uses Equation (2), revealing that the southern region is more resourceful than the northern. Particularly noteworthy are the zones with the most potential for development, including the city of Rongcheng in Weihai (100×10^7–120×10^7 kW), the sea area to the north of Weifang (80×10^7–100×10^7 kW), and the sea area to the south of Qingdao (60×10^7–90×10^7 kW). As shown in Figure 3b, Equation (8) was used to calculate the overall change characteristics, revealing that the sea area north of Weifang has the highest ST index as high as 1.3. Conversely, the ST index of the resources east of Rizhao is the lowest at about 0.6. It's noteworthy that there's a decreasing trend in the ST index of the two resources from north to south, indicating that the southern sea area is more conducive to the development and utilization of resources. As shown in Figure 3c, it is evident that the resource availability increases as one moves further away from the peninsula, with the highest percentage of availability still near the Weihai Rongcheng sea area (0.7–0.8). As shown in Figure 3d, this article focuses on the instantaneous CO coefficient (c (0)) [32], which is calculated using Equation (10). It is observed that the two resources exhibit complete CO in the northern sea area of Weifang, and they must coexist with a strong CO ($C(t) = 1$), which is due to the dominance of waves relative to winds. In contrast, other areas have a relatively small CO ($C(t) \leq 0.5$) with decreasing CO coefficients as one moves away from the shore, and the northern has a smaller CO coefficient than the southern. This leads to a reduction in the correspondence between the two resources, ensuring stable power output from the combined wave and wind farms. That is to say that if wave energy exceeds the maximum power generation, wind energy can make up for the demand for power output.

Based on the marine pastures application scenario, the range of potential development areas is between 10 and 30 km in accordance with Section 3.1.1. Because of the overlapping areas of different marine pastures, those with common areas grouped into large potential development areas (Figure 4). Considering the proximity of adjacent marine pastures, there is resource sharing between them, and the distribution of wave and wind energy resources is also generally similar. Therefore, we consider adjacent marine pastures as larger study areas. In this article, a total of seven larger study

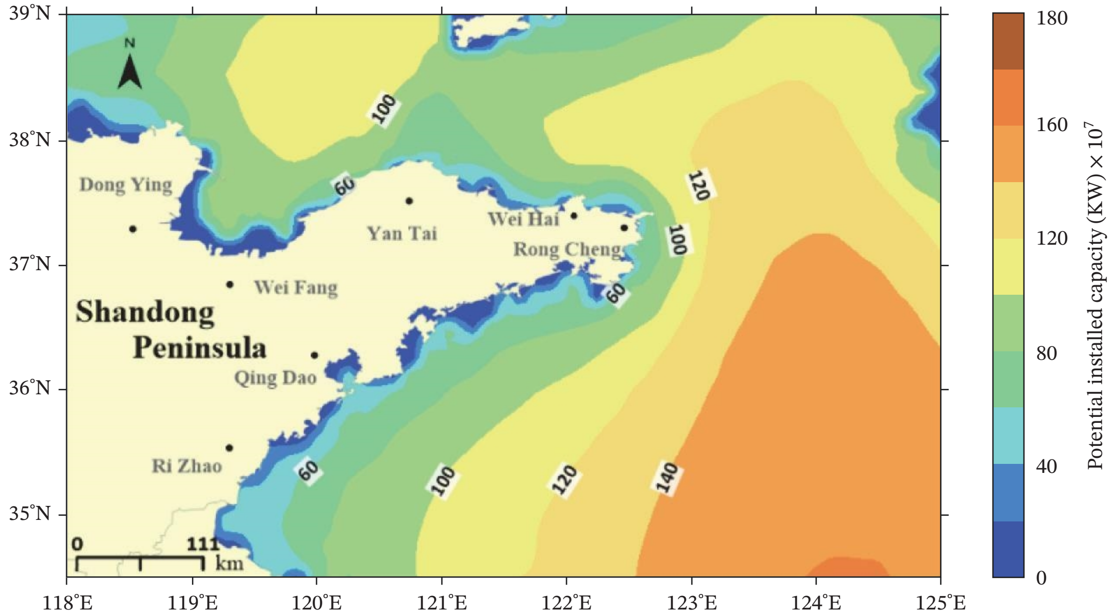

(a)

FIGURE 3 | (Continued)

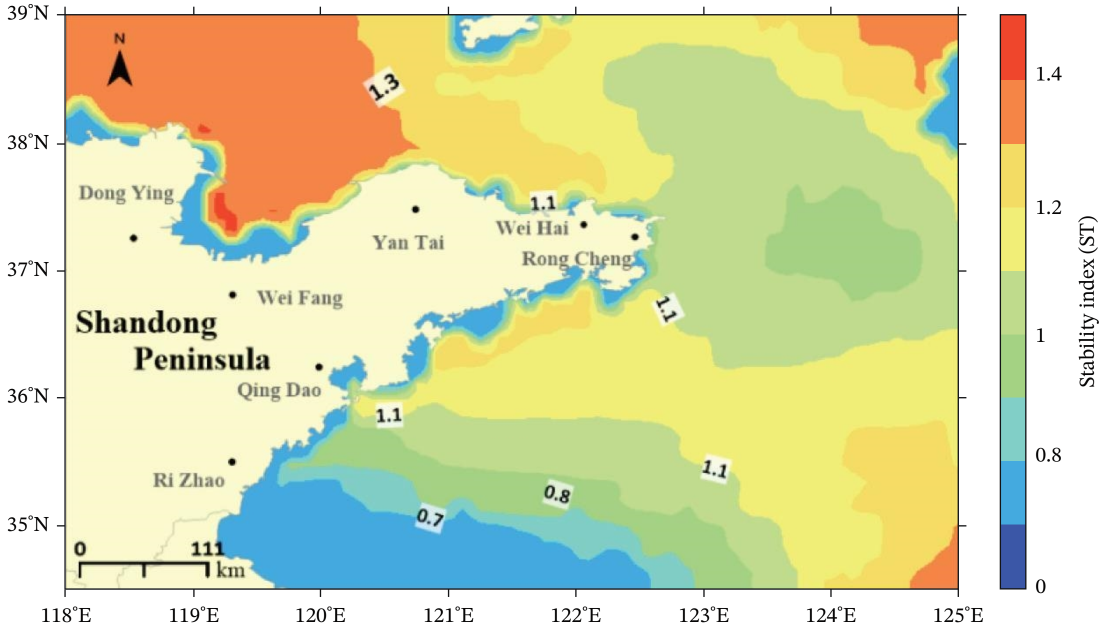

(b)

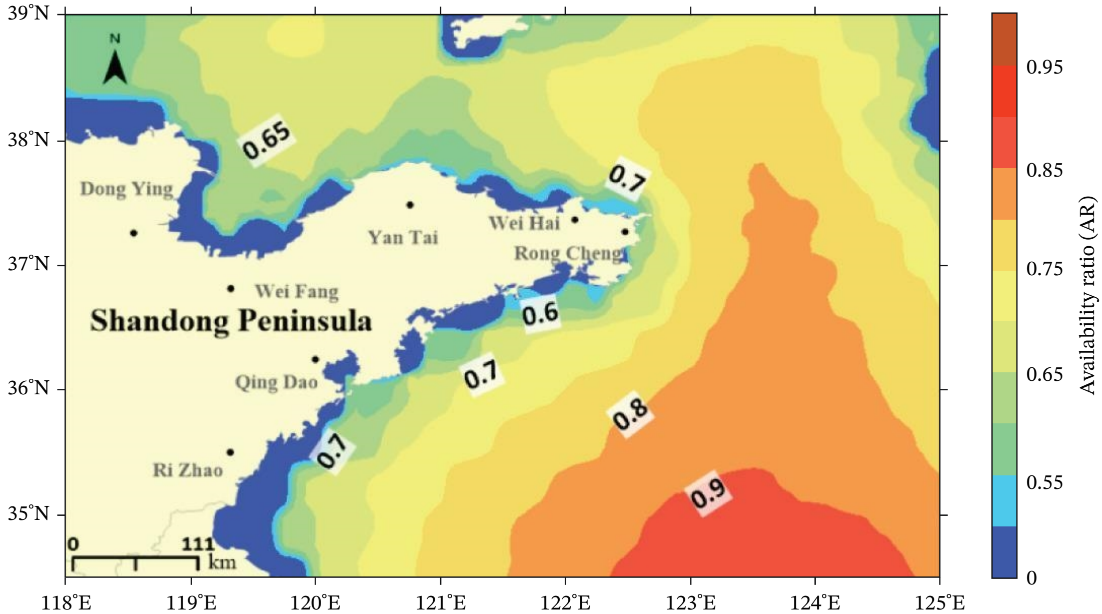

(c)

FIGURE 3 | (Continued)

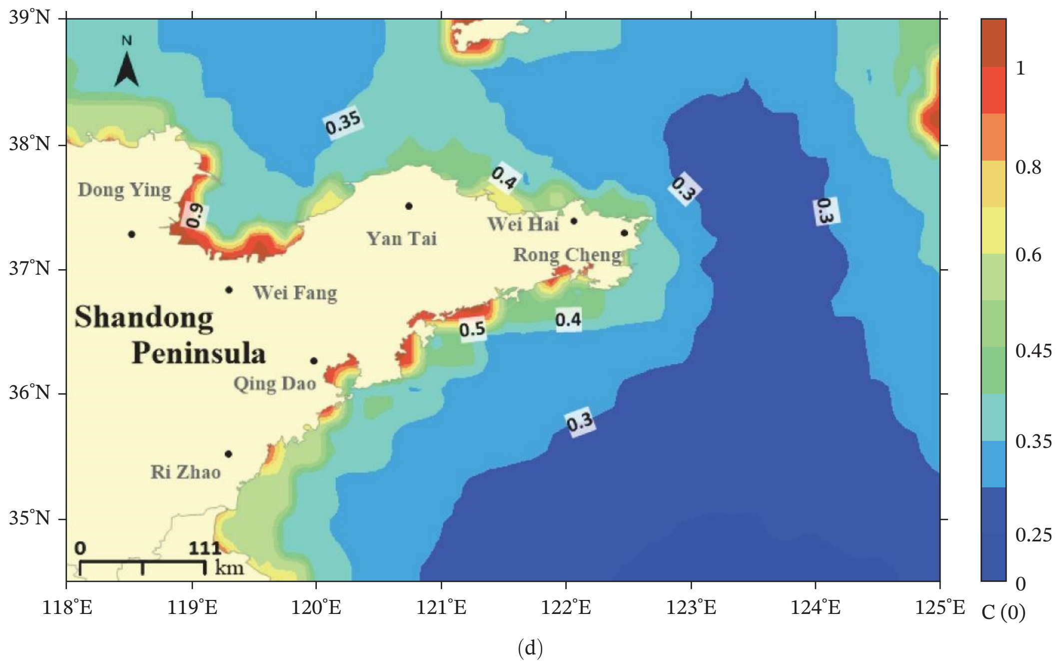

FIGURE 3 | Exploitable area: (a) total installed capacity (IC), (b) stability index (ST), (c) availability ratio (AR), and (d) correlation index (CO).

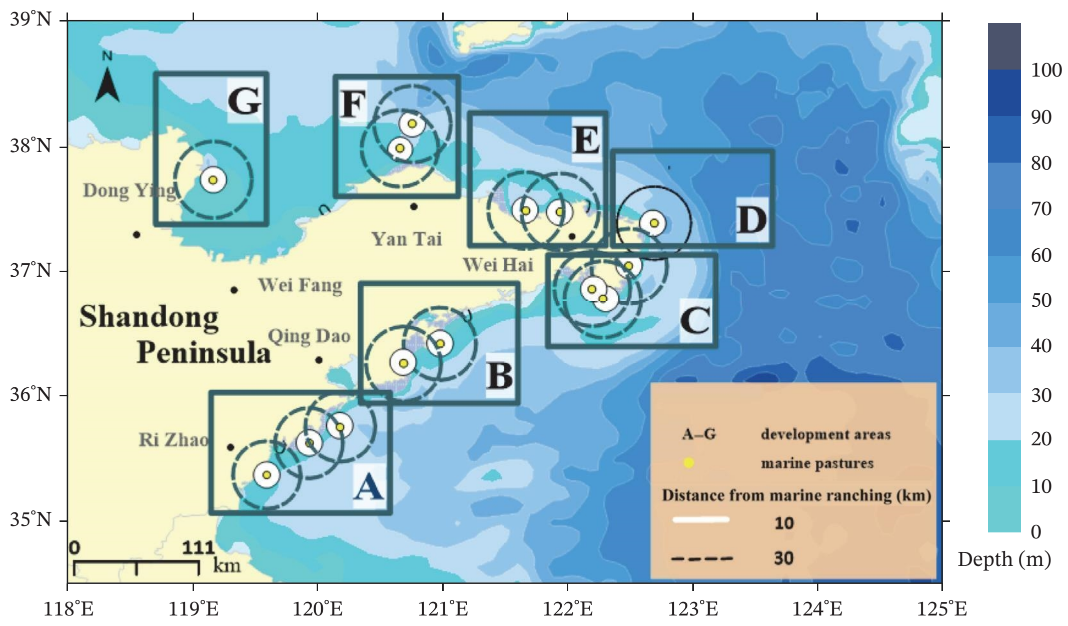

FIGURE 4 | Potential development area.

areas (A–G) were delineated. Among these areas, there are three marine pastures in areas A and C, two marine pastures in areas B and E, and one marine pasture in areas D and G. Within these larger study areas, we will select a site to deploy devices and provide power to all marine pastures. The benefit is better management of energy supply and the ability to share energy transmission infrastructure, thereby reducing construction and operational costs.

To select the most advantageous areas for developing the resources. The FUCOM methodology mentioned in Section 2.1 was used in this study. Smaller study sites measuring 0.125×0.125 were established in each larger study area. Within each larger study area, the JZC value of each smaller research site is calculated first, and then the sum of all JZC values of the smaller research sites is taken as the final result for that study areas. The number of smaller study sites within each larger study area was contingent upon the dimensions of the seven larger study area. To ensure comparability among study areas with the same research dimensions and to reduce biases introduced by differences in the number of sites, we separated the analysis into two groups based on different site quantities. This approach allows for a more accurate assessment of the characteristics and outcomes of each area. After calculating the 17 smaller sites in regions A, C, and F, and 11 sites in B, D, E, and G for evaluation, respectively, the weights of the four indexes in different potential

TABLE 3 | Weights of each indicator.

Potential development area	a	b	c	d	JZC
A	0.33	0.20	0.33	0.14	8.62
C	0.19	0.55	0.14	0.12	10.98
F	0.26	0.20	0.32	0.23	7.87
B	0.29	0.29	0.17	0.26	5.84
D	0.18	0.31	0.21	0.31	5.99
E	0.27	0.22	0.60	0.15	8.49
G	0.32	0.21	0.21	0.26	5.33

development areas can be calculated. The specific results (two decimal places reserved) are shown in Table 3.

The results show that C (JZC: 10.98) and A (JZC: 8.62) are selected among A, C, and F, D (JZC: 5.99) and E (JZC: 8.49) are selected among four areas, B, D, E, and G. Four areas, A, C, D, and E, were identified as critical development areas.

However, what we need more is to identify the most optimal sites for the deployment of WECs and WTs in the critical development areas. In thisarticle, we use the VIKOR method mentioned in Section 2.1 to rank all the smaller study areas in each of the dominant areas, prioritizing the locations. The different sites are named sequentially in order from top to bottom and left to right. The VIKOR method result value Q and the final location alternatives are shown in Table 4.

According to the ordering of each site in the four regions, this article selects one site as key site in each region respectively, which are A7 (119.75°N, 35.5°E), C6 (122°N, 36.75°E), D10 (122.5°N, 37.125°E), and E5 (121.5°N, 37.625°E). The specific locations are shown in Figure 5.

3.2 | The Synergy Between Offshore Wind and Wave Energy at the Key Sites

The synergy between the two resources reduces the uncertainty when relying on a single energy source and enhances the efficiency and reliability of energy utilization. The cross-CO factor quantifies the relationship between two resources. If there is a low CO or time lag between the two at zero time, utilizing the complementary advantages between the two can effectively reduce the variability in power output. As shown in Figure 6, the CO between wave height and wind speed at different times was calculated. It can be seen from the figure that the CO between the four stations at zero

TABLE 4 | Ranking of sites alternatives.

	A		C		D		E	
Region	Key sites	Q	Key sites	Q	Key sites	Q	Key sites	Q
Top1	A7	0.021	C6	0.000	D10	0.028	E5	0.000
Top2	A8	0.022	C7	0.007	D9	0.147	E8	0.443
Top3	A9	0.053	C10	0.014	D3	0.458	E9	0.444
Top4	A12	0.069	C11	0.025	D4	0.468	E6	0.852
Top5	A16	0.097	C12	0.029	D5	0.479	E1	0.855
Top6	A15	0.100	C8	0.128	D8	0.496	E7	0.858
Top7	A17	0.114	C13	0.134	D11	0.595	E2	0.859
Top8	A2	0.771	C9	0.141	D1	0.630	E3	0.862
Top9	A1	0.784	C14	0.146	D2	0.731	E11	0.863
Top10	A3	0.817	C3	0.156	D7	0.774	E10	0.995
Top11	A5	0.834	C4	0.158	D6	1.000	E4	0.999
Top12	A6	0.841	C2	0.211	—	—	—	—
Top13	A4	0.851	C5	0.224	—	—	—	—
Top14	A11	0.862	C15	0.287	—	—	—	—
Top15	A10	0.868	C16	0.300	—	—	—	—
Top16	A14	0.957	C17	0.304	—	—	—	—
Top17	A13	1.000	C1	1.000	—	—	—	—

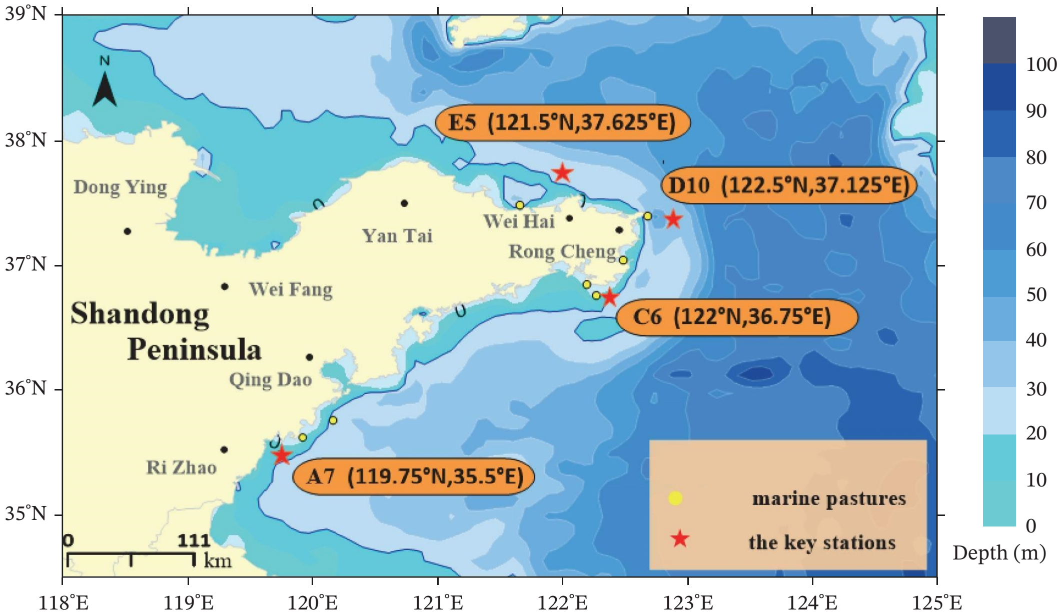

FIGURE 5 | Key site location.

time is low, with the lowest observed at E5 sites. All stations have a time delay phenomenon and reach the maximum value around 4 h, before gradually decreasing over time.

In addition, wind and wave direction are critical for the deployment of WECs and WTs, ensuring optimal capture of corresponding energy. Wind rose diagrams and wave rose diagrams were employed to analyze the directional patterns of wave energy and wind power density distribution at four sites (Figure 7). As depicted, at site D10, more than 20% of wave energy is concentrated in the north (N), while at the remaining three sites, energy is mainly concentrated in the south (S) and south–southeast (SSE). Among these, Site A7 has a relatively concentrated energy distribution, but Site C6 has a more dispersed distribution, with a maximum value of only 16%. Regarding wind speeds, at all sites, wind energy exceeding 20% predominantly originates from the north (N) or north–northwest (NNW). Except for D10, the wave energy and wind energy directions at the other three sites at the same location are not consistent, which brings the benefit that devices can absorb energy from multiple directions.

Wave condition analysis is pivotal in wave and wind energy development, enhancing energy capture efficiency and equipment safety. Scatter plots for waves (Figure 8a) and energy curves for wind (Figure 8b) were generated. In Figure 8a, the color scale represents percentages, with colors corresponding to different percentages, and the numbers indicate the frequency of occurrences per year within various wave height and wave period ranges. The most

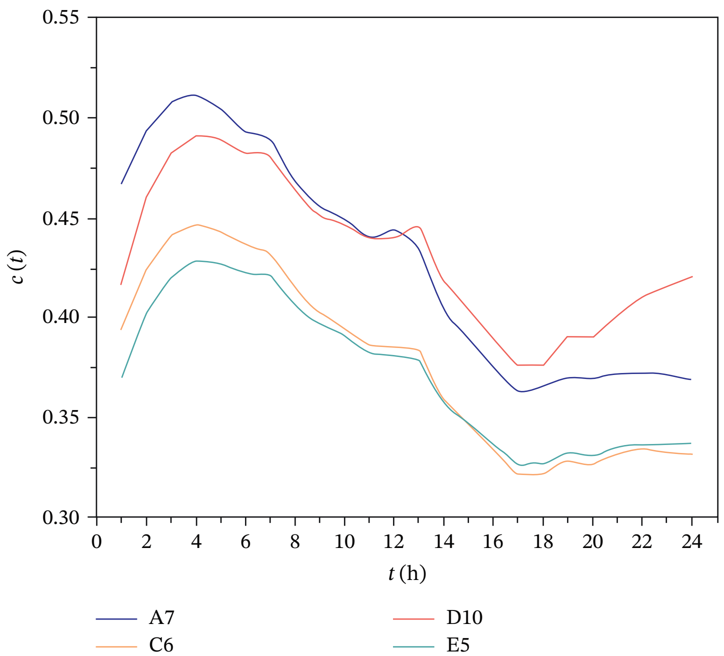

FIGURE 6 | The cross-correlation between significant wave height (Hs) and wind speed (V) and t the time lag.

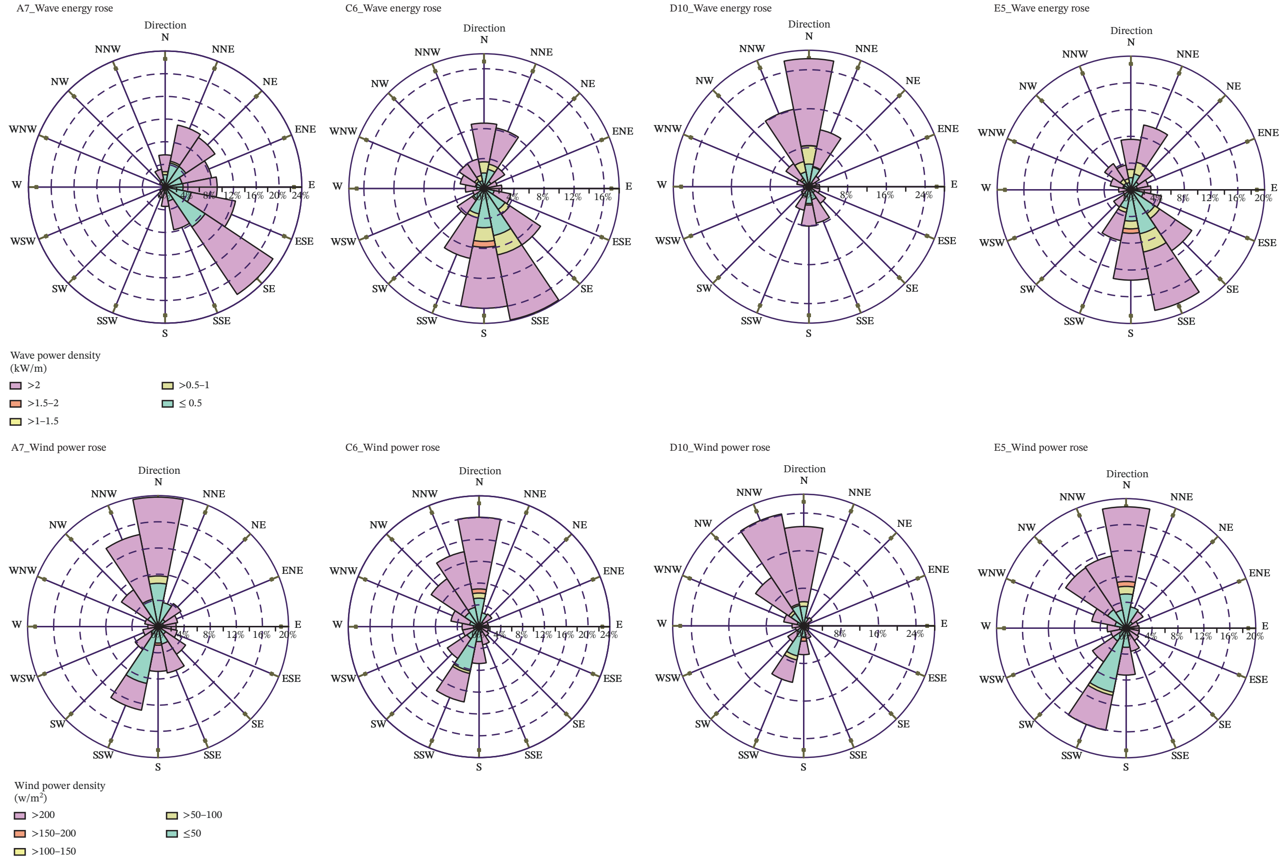

FIGURE 7 | Wave energy rose, and wind power rose for each key site.

common sea conditions have Hs ranging from 0 to 2.5 m and Te ranging from 3 to 8 s. Additionally, sea conditions with Hs between 1 and 2 m and Te between 4 and 6 s contribute more than 12% to the total wave energy distribution (Figure 8a). From Figure 8b, it can be observed that at the selected location, the most common wind speeds range from 6 to 12 m/s (>20%). This wind condition contributes more than 30% to the total wind energy distribution.

The availability of these two energy sources in different seasons can be understood by analyzing the monthly average wave energy flux and wind power density. As shown in Figure 9, for wind power, all four sites are most active in January, February, October, November, and December, exceeding 0.5 kW/m^2. For wave energy resources, site D10 shows a similar phenomenon, exceeding 10 kW/m^2. For the other three sites, the most active seasons for wave energy resources are in July and August and November and December.

3.3 | Determining the Optimal Device and Power Generation With Different Combinations at the Key Sites

This article employed the average power output and the capacity factor to determine the most suitable WECs and WTs (Equations (11)–(14)). First, we determine the most appropriate WECs, and the results of the suitability evaluation indexes of each device on the key site are shown in Table 5. This article takes into account devices that are suitable for the specific water depth at each site, where symbols "——" indicate that the water depth of the sites is not suitable for WECs. The highest average power output and capacity factor was obtained for Wave Star at all sites, with the average power outputs were 46.92 kW, 65.39 kW, 69.99 kW, and 63.99 kW, respectively, and the capacity factors were 7.82%, 10.09%, 11.67%, and 10.67%, respectively. Thus, Wave Star was the most appropriate WEC for all sites.

The most suitable WTs are determined, and the results of the suitability evaluation indexes of WTs on the key sites are shown in Table 6. The highest average power output and capacity factor was obtained for the SIEMENS (SWT-7.0-154) in sites A7, C6, and E5, where the average power output was 432.40 kW, 63.99 kW, and 645.40 kW, respectively, the capacity factor was 7.19%, 13.03%, and 13.33%, respectively. When assessing capacity factor at site D10, ENVISION (EN130-4.2) appears to be the optimal device, with a capacity factor of 23.01%. When assessing average power output, VESTAS (V164 8 MW) appears to be the optimal device, with an average power output of 1256.80 kW. Similarly, the site has lower capacity factor values, so priority is given to average power output. Finally, SIEMENS (SWT-7.0-154) was the most suitable WTs at sites A7 C6, and E5, and VESTAS (V164 8 MW) was the most suitable WTs at sites D10.

After the WEC and WT are deployed at the key sites, one of the key points to focus on is the distribution of power generation. If the equipment is consistently operating at low power output, its utility value significantly decreases. Therefore, it is necessary to analyze the duration of time that a certain power output is generated.

In this study, the analysis method involves determining the IC for four sites, according to the inter-annual generation capacity of one marine pasture as specified in Section 2.2.2, the total IC of areas A,

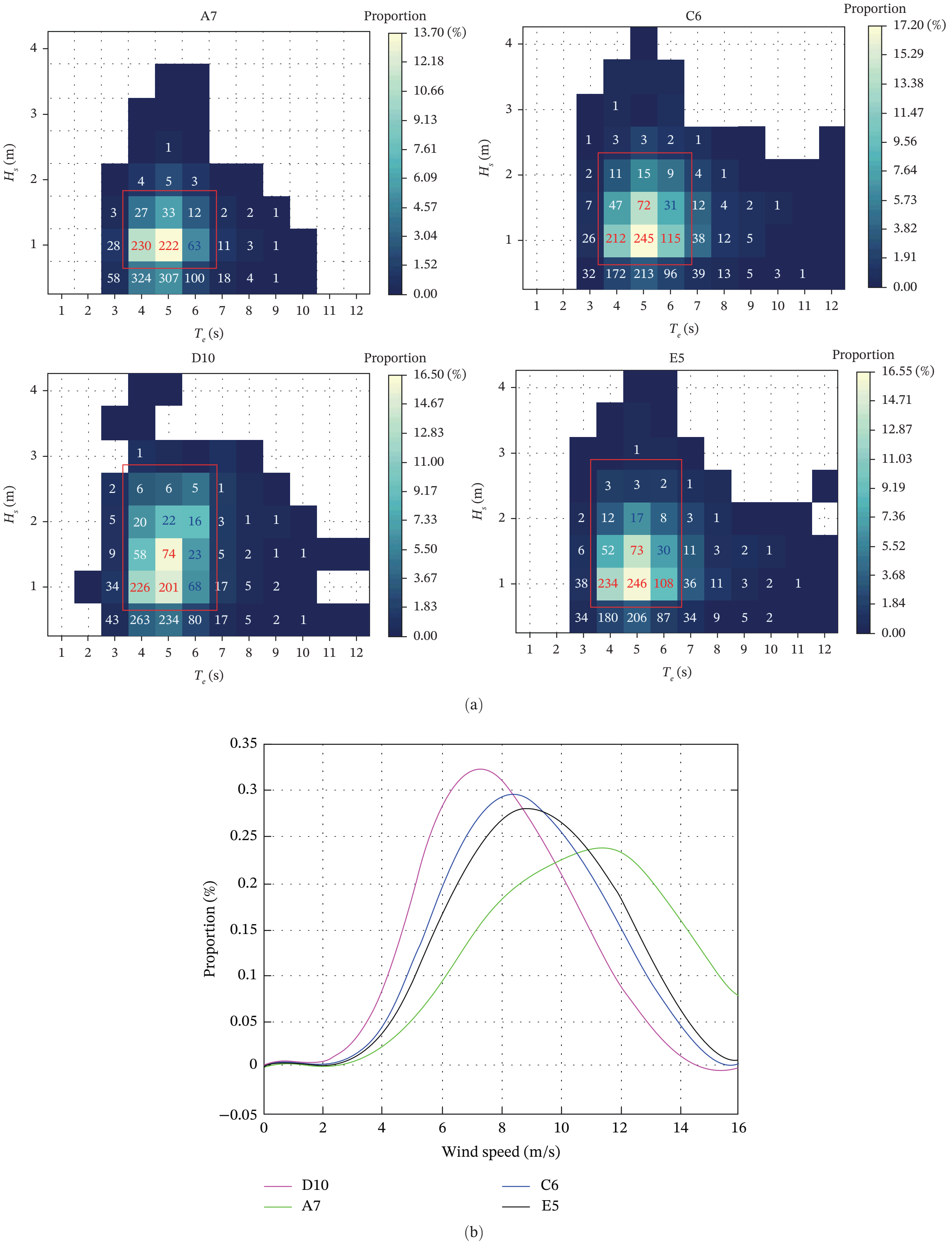

FIGURE 8 | (a) Distributions of total wave energy flux according to significant wave height and wave period for each site. (b) Curve denoting wind speed and the corresponding wind energy density.

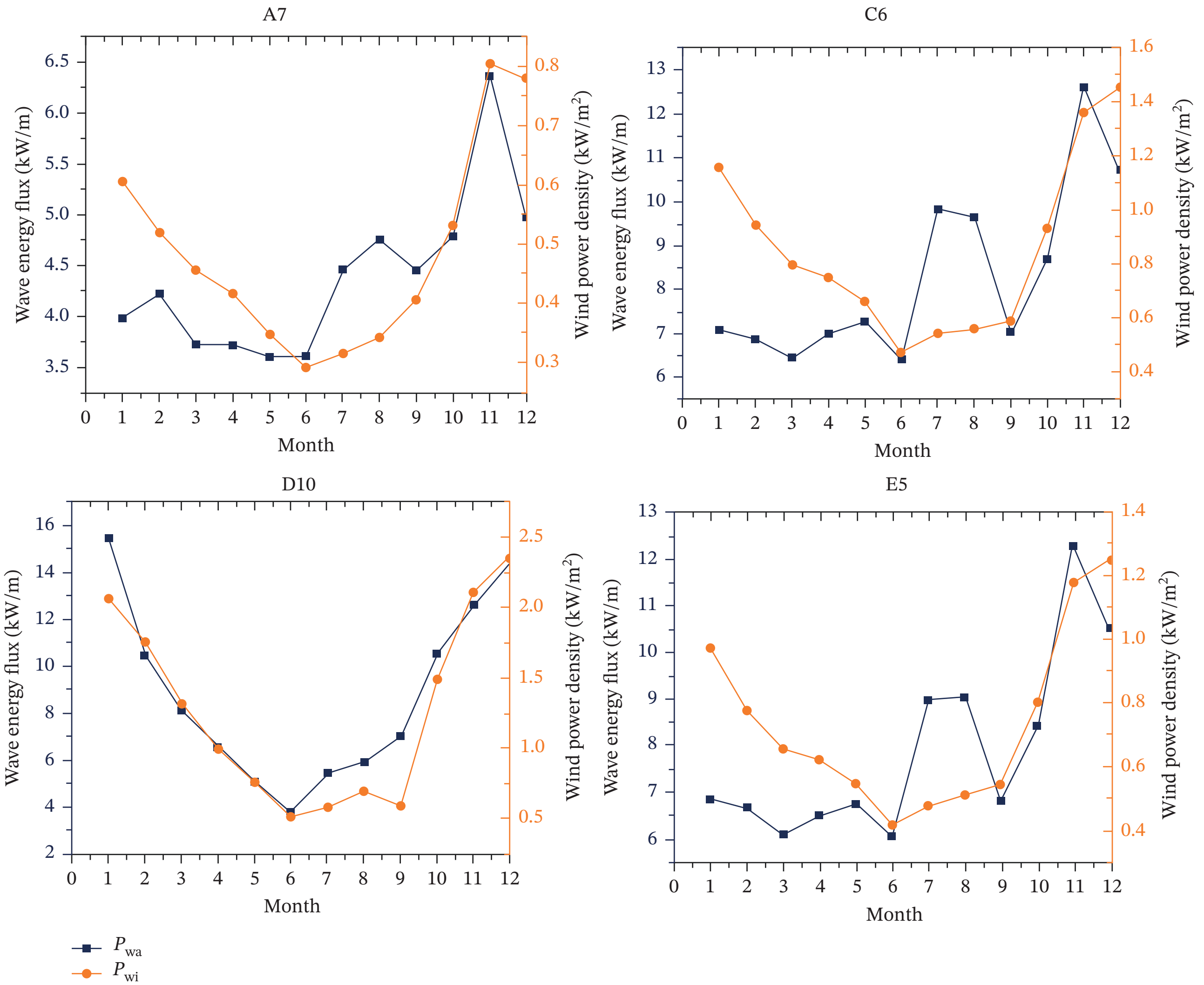

FIGURE 9 | Monthly mean of P_{wa} and P_{wi} at four sites.

C, D, and E was specified as 84 MW, 84 MW, 42 MW, and 84 MW, respectively. Then six different scenarios (com1–com6) for the share of two resources are identified. The first combination (com1) consists of 100% wave energy capacity (independent wave farm), and the last combination (com6) consists of 100% wind energy capacity (independent wind farm). In the remaining combinations (com2–com5), wave energy is increased by 20%, and wind energy is reduced by 20%. Finally, we analyze the time proportion of power production for different combinations. The results of the calculations for each site is shown in Figure 10.

The x-axis represents six different combinations, and the y-axis represents the proportion of time that specific power outputs occur. Each combination is depicted with a bar graph showing specific power

TABLE 5 | Evaluation indicators for WECs.

WECs	A7	C6	D10	E5
Wave Star				
P_{e_wa} (kW)	46.92	65.39	69.99	63.99
C_{f_wa} (%)	7.82	10.9	11.67	10.67
Oyster				
P_{e_wa} (kW)	6.13	12.57	23.33	12.54
C_{f_wa} (%)	0.77	1.57	2.92	1.57
CETO				
P_{e_wa} (kW)	—	9.07	10.18	8.96
C_{f_wa} (%)	—	3.49	3.92	3.44

TABLE 6 | Evaluation indicators for WTs.

WTs	A7	C6	D10	E5
SIEMENS				
P_{e_wi} (kW)	432.40	749.30	1099.70	645.40
C_{f_wi} (%)	7.19	13.02	17.26	13.33
VESTAS				
P_{e_wi} (kW)	494.20	856.30	1256.80	737.60
C_{f_wi} (%)	5.39	10.92	19.54	9.02
ENVISION				
P_{e_wi} (kW)	328.70	562.40	799.50	487.00
C_{f_wi} (%)	8.72	15.65	23.01	11.02

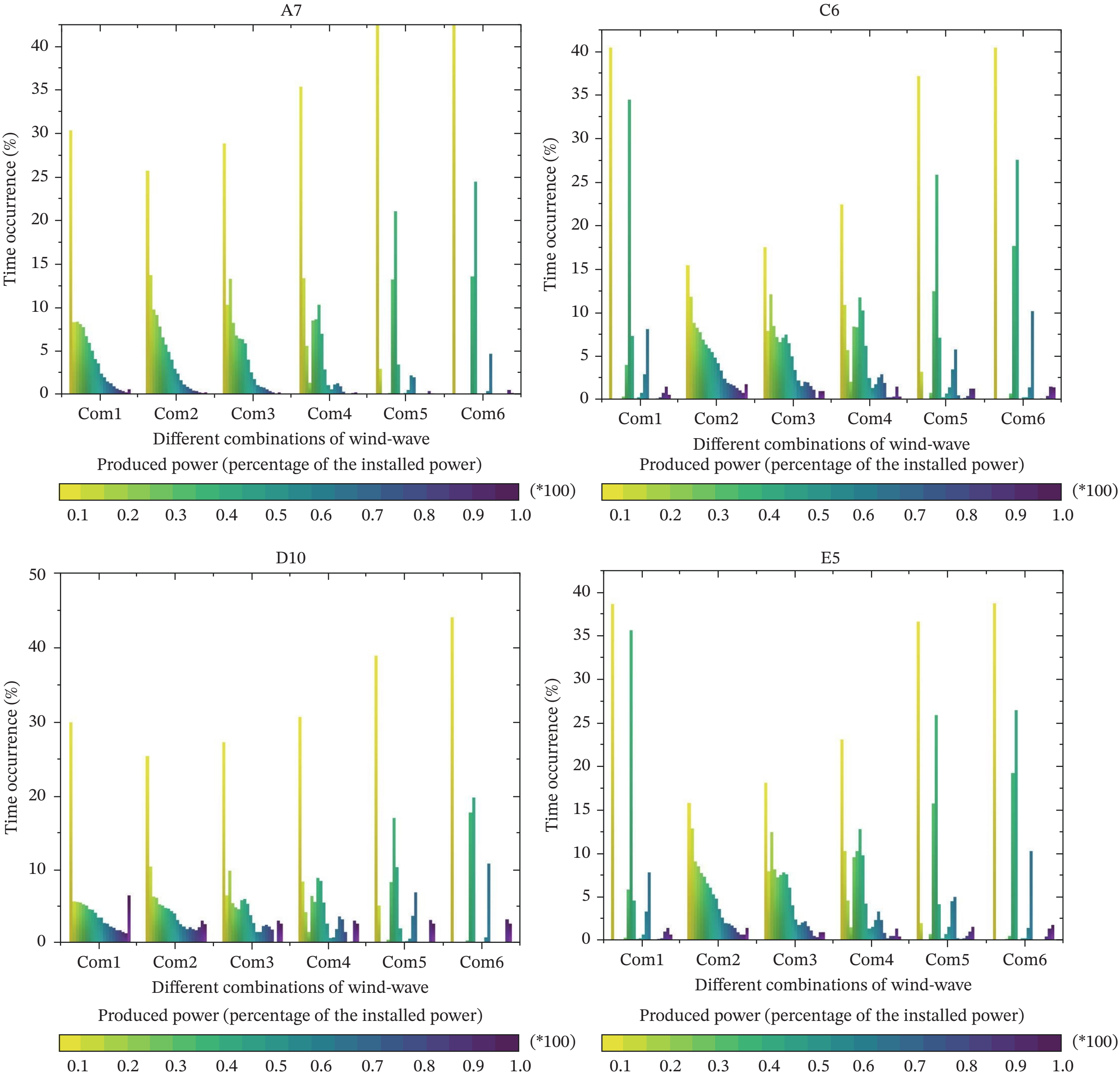

FIGURE 10 | Time distribution of the power produced.

outputs ranging from 0 to 100% of the IC. The graph illustrates that compared to standalone wave and wind power plants, combined wave and wind power plants can effectively reduce low-capacity power outputs (0%–10%). This reduction is most evident at sites C6 and E5, where the Com2 combination decreases the low-capacity output by 25% and 22%, respectively. Additionally, in wind farms, certain specific power outputs have a duration of zero; by incorporating wave energy, power output at all levels can be achieved.

4 | Conclusions

This study analyzed the potential for combined development of wave energy and wind energy in the coastal areas around the Shandong Peninsula over the past 15 years. Evaluation indicators were established to assess the combined resources of two. Based on this indicator along with considerations of site distances, a methodology for selecting station location is proposed. Meanwhile, a cooperative operational mode for the two resources was examined based on their distribution. Furthermore, the distribution of power generation times for various combinations of WEC and WT at each site was analyzed. The conclusions are as follows:

1. This article proposes a unified criterion to assess the abundance situation of wave and wind energy. This addresses a key limitation of previous studies that relied on disparate evaluation systems. Finally, constructing JZC based on four metrics of potential IC, stability, AR, and CO, using the FUCOM method in the Shandong Peninsula national-level marine pasture. The JZC, with its innovative inclusion of indicator weights derived from FUCOM and consideration of optimal station construction distance, significantly enhances the precision and applicability of site selection. It can identify potential development areas. Through analysis, Qingdao and Weihai are more advantageous for the development of both types of energy. Among them, regions A, C, D, and E are the preferred areas for joint development of wave and wind energy resources. Second, to determine the optimal sites for powering all marine pasture within each potential development areas, this study employs the VIKOR method to identify the most suitable sites for installing devices. This approach effectively balances multi-criteria conflicts, leading to robust and practical site recommendations. Through analysis, site A7 (119.75°N, 35.5°E) is preferred for marine ranches of Ruizi, the Sea Area of Qingdao Zhaitang Island (01), Taoshengyijiu, the Sea Area of Qingdao Lingshan Bay (02) and Taoshengyijiu, the Sea Area of Qingdao Lingshan Bay (03). Site C6 (122°N, 36.75°E) is preferred for marine pasture of Xinhong the Sea Area of Rocheng Jinghai Bay (06), Taoyuan, the Sea Area of Rongcheng Sushan Island (07) and Dongxing, the Sea Area of Rocheng Boge Island (08). Site D10 (122.5°N, 37.125°E) is preferred for marine ranch of the Sea Area of Rocheng Chudao Island (09). Site E5 (121.5°N, 37.625°E) is preferred for marine ranch of Yutai the Sea Area of Weihai ShuangdaoBay (10) and Kongji Eastern Sea Area of Yantai Yangma Island (11). Installing wave and wind energy devices at these four sites will supply power to all marine pasture within each advantageous area, maximizing resource utilization.
2. At four sites, the two resources exhibit low CO and a 4-h time lag, which will be beneficial for a more stable power output when the resources are combined. The monthly volatility of these two resources at key sites is high, with October, November, and December being the most active months for these two resources. The most prevalent wave direction is southward, while the most prevalent wind direction is northward. Additionally, the key sites have a significant wave height (Hs) between 1 and 2 m and wave energy period (Te) between 4 and 6 s, while wind speeds 6–12 m/s are the most frequent.
3. Wave Star is identified as the most suitable WEC for deployment at four sites. For WT, Siemens (SWT-7.0–154) is the most appropriate for sites A7, C6, and E5, while Vestas (V164 8MW) is most suitable for site D10. Compared to a standalone wave or wind farm, specific proportions of installed wave and wind energy capacity can effectively reduce the occurrence of low power periods across the entire energy field.

5 | Discussion

This article selects the most suitable site for the joint development of wave and wind energy in marine pastures off the Shandong Peninsula and analyzes the optimal development model for devices at this site. Compared to existing evaluations of these two energy sources conducted separately, the overall resource distribution trends are similar [14–16]. However, our work significantly advances previous research by addressing several critical limitations. With environmental preservation as a priority. We standardized the evaluation criteria, conducted an in-depth analysis of the benefits brought by the combination of the two energy sources, and, by considering specific application scenarios, conducted a comprehensive analysis of various indicators. By constructing a JZC, we further optimized the scientific selection of energy sites and ultimately proposed a more targeted and practical solution. This integrated approach offers a more holistic understanding of resource development potential, moving beyond conventional individual resource assessments.

However, the limitations of this work should not be overlooked. In future research, efforts should focus on optimizing the operational and maintenance costs of wave and wind power plants, as well as the planning of infrastructure to improve economic efficiency. At the same time, research and development of related technologies and supporting equipment should be prioritized, alongside strengthening fault prediction capabilities and improving maintenance efficiency. Furthermore, the introduction of advanced data processing algorithms, such as machine learning or deep learning, should be emphasized to further enhance the scientific level of site selection.

Author Contributions

Yong Wan and Qiuwei Cheng: conceptualization, validation. **Qiuwei Cheng**: methodology, writing – original draft preparation. **Xiaoshun Feng**: data curation, visualization. **Yong Wan**: writing – review and editing. **Yongshou Dai**: supervision.

Acknowledgments

The authors would like to convey their appreciation to the editors and anonymous reviewers for their insightful remarks and constructive feedback on this manuscript.

Funding

The study was supported by the National Natural Science Foundation of Shandong Province (Grant ZR2022ME039), the National Natural Science Foundation of China (Grant 61931025), and the National Natural Science Foundation of China (NSFC), “Deep Learning-based Seismic Wave Extraction Methods for Deep Earth Pre-stack Time Spatial Domain” (Grant 42274159).

Disclosure

All authors have read and agreed to the published version of the manuscript.

Conflicts of Interest

The authors declare no conflicts of interest.

Data Availability Statement

Thanks to the National Data Buoy Center for buoy data and the European Center for Medium and Long-term Weather Forecasts for ECMWF ERA5 data.

References

1. D. Clemente, F. Teixeira-Duarte, P. Rosa-Santos, and F. Taveira-Pinto, “Advancements on Optimization Algorithms Applied to Wave Energy Assessment: An Overview on Wave Climate and Energy Resource,” *Energies* 16, no. 12 (2023): 4660.

2. Ş. Kılkış, G. Krajačić, N. Duić, M. A. Rosen, and M. A. Al-Nimr, “Effective Mitigation of Climate Change With Sustainable Development of Energy, Water and Environment Systems,” *Energy Conversion and Management* 269 (2022): 116146.

3. B. Battisti, G. Bracco, and M. Bergmann, “A Multi-Fidelity Model for Wave Energy Converters,” *International Journal for Numerical Methods in Fluids* 97, no. 4 (2025): 427–445.

4. C. Kalogeri, G. Galanis, C. Spyrou, et al., “Assessing the European Offshore Wind and Wave Energy Resource for Combined Exploitation,” *Renewable Energy* 101 (2017): 244–264.

5. Y. Wang, S. Huang, G. Xue, and Y. Liu, “Influence of Hydraulic PTO Parameters on Power Capture and Motion Response of a Floating Wind-Wave Hybrid System,” *Journal of Marine Science and Engineering* 10, no. 11 (2022): 1660.

6. M. M. Nezhad, A. Heydari, M. Neshat, F. Keynia, G. Piras, and D. A. Garcia, “A Mediterranean Sea Offshore Wind Classification Using MERRA-2 and Machine Learning Models,” *Renewable Energy* 190 (2022): 156–166.

7. P.-H. Gonzalo, H. Luka, and P. Antun, “Capturing Features of Hourly-Resolution Energy Models Through Statistical Annual Indicators,” *Renewable Energy* 197 (2022): 1192–1223.

8. I. M. Solbrekke and A. Sorteberg, “Norwegian Offshore Wind Power—Spatial Planning Using Multi-Criteria Decision Analysis,” *Wind Energy* 27, no. 1 (2024): 5–32.

9. D. S. A. Rayhan and I. U. Bhuiyan, “A Framework for Evaluation of Construction and Demolition Waste Management Alternatives Using MCDA Techniques in the Context of Dhaka City,” *International Journal of Construction Management* 25, no. 4 (2025): 481–493.

10. S. Değirmenci, F. Bingöl, and S. C. Sofuoglu, “MCDM Analysis of Wind Energy in Turkey: Decision Making Based on Environmental Impacts,” *Environmental Science and Pollution Research* 25, no. 20 (2018): 19753–19766.

11. S. Hall, “GIS-Based Multi-Criteria Decision Analysis for Marine Energy Site Selection: A Case Study Comparison Between Puerto Rico and Hawaii,” (2024).

12. M. Mahdy and A. S. Bahaj, “Multi Criteria Decision Analysis for Offshore Wind Energy Potential in Egypt,” *Renewable Energy* 118 (2018): 278–289.

13. P. A. Adedeji, S. A. Akinlabi, N. Madushele, and O. O. Olatunji, “Neuro-Fuzzy Resource Forecast in Site Suitability Assessment for Wind and Solar Energy: A Mini Review,” *Journal of Cleaner Production* 269 (2020): 122104.

14. L. Rusu, D. Ganea, and E. Mereuta, “A Joint Evaluation of Wave and Wind Energy Resources in the Black Sea Based on 20-Year Hindcast Information,” *Energy Exploration & Exploitation* 36, no. 2 (2018): 335–351.

15. A. Azzellino, C. Lanfredi, L. Riefolo, V. De Santis, P. Contestabile, and D. Vicinanza, “Combined Exploitation of Offshore Wind and Wave Energy in the Italian Seas: A Spatial Planning Approach,” *Frontiers in Energy Research* 7 (2019): 42.

16. F. Ferrari, G. Besio, F. Cassola, and A. Mazzino, “Optimized Wind and Wave Energy Resource Assessment and Offshore Exploitability in the Mediterranean Sea,” *Energy* 190 (2020): 116447.

17. A. Lira-Loarca, F. Ferrari, A. Mazzino, and G. Besio, “Future Wind and Wave Energy Resources and Exploitability in the Mediterranean Sea by 2100,” *Applied Energy* 302 (2021): 117492.

18. Q. Gao, S.S. Khan, N. Sergiienko, et al., “Assessment of Wind and Wave Power Characteristic and Potential for Hybrid Exploration in Australia,” *Renewable and Sustainable Energy Reviews* 168 (2022): 112747.

19. L. Rusu, “An Evaluation of the Synergy Between the Wave and Wind Energy Along the West Iberian Nearshore,” *Energy Conversion and Management: X* 20 (2023): 100453.

20. T. Görmüş, B. Aydoğan, and B. Ayat, “Analysis of Hybrid Exploitation of Wind and Wave Power in the Mediterranean and the Black Sea,” *Energy Conversion and Management* 299 (2024): 117820.

21. M. Huiqun and W. Qifeng, “Wind Energy Resource Assessment for Shandong Province,” in *World Automation Congress*, (Puerto Vallarta, 2012): 1–4.

22. Y. Wan, C. Q. Fan, and Y. S. Dai, “A Study on the Potential Development of Wave Energy in the Coastal Waters Around the Shandong Peninsula,” *Journal of Solar Energy* 39, no. 12 (2018): 3311–3318.

23. S. Liu, Z. Yang, and Y. Xinyang, “Wave Energy Resource Assessment in Shandong Offshore,” *Haiyang Xuebao* 37, no. 7 (2015): 108–122.

24. D. G. Vagiona and M. Kamilakis, “Sustainable Site Selection for Offshore Wind Farms in the South Aegean—Greece,” *Sustainability* 10, no. 3 (2018): 749.

25. W. Yong, F. Chenqing, and D. Yongshou, “Wave Energy Development Potential Assessment in Nearshore Sea Area Around Around Shandong Peninsula,” *Acta Energiae Solaris Sinica* 39, no. 12 (2018): 3311–3318.

26. H. Shi, X. Cao, Q. Li, et al., “Evaluating the Accuracy of ERA5 Wave Reanalysis in the Water Around China,” *Journal of Ocean University of China* 20, no. 1 (2021): 1–9.

27. Y. Wan, C. Fan, Y. Dai, et al., “Assessment of the Joint Development Potential of Wave and Wind Energy in the South China Sea,” *Energies* 11, no. 2 (2018): 398.

28. K. Wang, D. Wu, J. Wu, et al., “Wind Energy Resources at Antarctic Stations Based on ERA5,” *Atmosphere* 14 (2023): 1732.

29. D. Pamučar, Ž. Stević, and S. Sremac, “A New Model for Determining Weight Coefficients of Criteria in MCDM Models: Full Consistency Method (FUCOM),” *Symmetry* 10, no. 9 (2018): 393.

30. C.-L. Chang, “A Modified VIKOR Method for Multiple Criteria Analysis,” *Environmental Monitoring and Assessment* 168, no. 1–4 (2010): 339–344.

31. Y. Wan, C. Zheng, and L. Li, “Wave Energy Assessment Related to Wave Energy Convertors in the Coastal Waters of China,” *Energy* 202 (2020): 117741.

32. E. Gaughan and B. Fitzgerald, "An Assessment of the Potential for Co-Located Offshore Wind and Wave Farms in Ireland," *Energy* 200 (2020): 117526.

33. Y. Y. Kong and M. Y. Wang, "The First Semi Submersible Wave Energy Aquaculture Cage in China Delivered in Guangdong," *Ocean and Fishery* 08 (2019): 74–75.

34. V. Vannucchi and L. Cappietti, "Wave Energy Assessment and Performance Estimation of State of the Art Wave Energy Converters in Italian Hotspots," *Sustainability* 8, no. 12 (2016): 1300.

35. R. A. Gideon and E. Bou-Zeid, "Collocating Offshore Wind and Wave Generators to Reduce Power Output Variability: A Multi-Site Analysis," *Renewable Energy* 163 (2021): 1548–1559.

Appendix A

The FUCOM method's basic steps are as follows:

The following are the steps for the calculation of FUCOM: where $C_1C_2C_3C_4$ represent the four indicators of richness, potential installed capacity, stability, the availability ratio, and the correlation.

Step 1: Ranking of predefined indexes $C = \{C_1, C_2, \ldots\ldots, C_n\}$

The ranking is based on the highest significance of the criterion to the lowest, therefore, the criterion of ranking according to the expected value of the weight coefficients, the equation is shown:

$$C_{j(1)} \geq C_{j(2)} \geq \ldots \geq C_{j(\mathrm{p})} \tag{A.1}$$

where $j$denotes the priority.

The predefined ranking of indicators for each region is $\mathrm{C(A)} = \{C_3, C_1, C_2, C_4\}\mathrm{C(B)} = \{C_3, C_1, C_2, C_4\}$, $\mathrm{C(C)} = \{C_2, C_1, C_3, C_4\}$, $\mathrm{C(D)} = \{C_3, C_1, C_2, C_4\}$, $\mathrm{C(E)} = \{C_3, C_1, C_2, C_4\}$, $\mathrm{C(F)} = \{C_3, C_1, C_4, C_2\}$, $\mathrm{C(G)} = \{C_1, C_4, C_2, C_3\}$

Step 2: Prioritize comparisons of evaluation criteria between attributes $\phi_{p/(p+1)}, p = 1 \ldots N$

The comparison priority equation for the evaluation criterion $\phi_{p/(p+1)} = C_{j(p)}/C_{j(p+1)}$. The comparison is scaled by mapping the data between [1,9], which ultimately leads to a comparison priority vector of evaluation criteria with the expression shown:

$$\phi = \left(\phi_{\frac{1}{2}}, \phi_{\frac{2}{3}}, \ldots, \phi_{\frac{p}{p+1}}\right) \tag{A.2}$$

The value of ϕ for each region $\phi(\mathrm{A}) = (1, 1.67, 1.4)$, $\phi(\mathrm{B}) = (2, 1, 1)$, $\phi(\mathrm{C}) = (3, 1.33, 1.13)$, $\phi(\mathrm{D}) = (1, 1.5, 1.17)$, $\phi(\mathrm{E}) = (1.33, 1.25, 1.4)$, $\phi(\mathrm{F}) = (1.20, 1.17, 1.14)$, $\phi(\mathrm{G}) = (1.25, 1.20, 1)$

Step 3: Calculate the final value of the evaluation criteria weight $(w_1, w_2, \ldots, w_n)^T$

The conditions satisfied by the weighting factors are as follows:

$$\frac{w_p}{w_{(p+1)}} = \phi_{\frac{p}{p+1}} \tag{A.3}$$

$$\frac{w_p}{w_{(p+2)}} = \phi_{\frac{p}{p+1}} \otimes \phi_{\frac{k+1}{k+2}} \tag{A.4}$$

Determine the final model based on the defined (A.5)

$$\begin{aligned} &\min\chi \\ &\left|\frac{v_j(p)}{w_j(p+1)} - \varphi_{\frac{p}{p+1}}\right| \leq \chi, \forall j \\ &\left|\frac{v_j(p)}{w_j(p+2)} - \varphi_{p/(p+1)} \otimes \varphi_{(p+1)/(p+2)}\right| \leq \chi, \forall j \\ &\sum_{j=1}^{n} w_j = 1, \forall j \\ &w_j \geq 0, \forall j \end{aligned} \tag{A.5}$$

Based on the above constraints on the optimal value, the weights for the four indicators are determined in the end. The potential development areas are finally selected.

Appendix B

A VIKOR method's basic steps are as follows:

Step 1: Standardize the data and identify the ideal solution.

Beneficial indexes:

$$r_{ij} = \frac{a_{ij}}{\sqrt{\sum_{i=1}^{m} a_{ij}^2}} \tag{B.1}$$

Costly indexes:

$$r_{ij} = \frac{\frac{1}{a_{ij}}}{\sqrt{\sum_{i=1}^{m} (1/a_{ij})^2}} \tag{B.2}$$

a_{ij} is the jth evaluation indexes in the ith sites. In this paper, the positive ideal solution and the negative ideal solution are both specified as 1: $f_j^- = 1$, $f_j^+ = 1$

Step 2: Calculate the group benefit value and individual regret value.

Take the positive ideal solution as an example:

$$\begin{aligned} &S_i^+ = \sum_{j=1}^{n} \omega_j \frac{f_j^+ - r_j}{f_j^+ - f_j} \\ &i = 1, 2, \ldots, m;\ j = 1, 2, \ldots, n_e \\ &R_i^+ = \max \omega_j f_j^+ - f_j^- \\ &i = 1, 2, \ldots, n_s \end{aligned} \tag{B.3}$$

largest group utility and the smallest individual:

$$\begin{aligned} &S_i = \frac{S_i^+}{S_i} \\ &i = 1, 2, \cdots, m_s \\ &R_i = \frac{R_i^+}{R_i} \\ &i = 1, 2, \cdots, m_s \end{aligned} \tag{B.4}$$

Step 3: Calculate the ratio. a denotes the compromise coefficient ($a = [0{,}1]$), which is taken as $a = 0.5$ in this paper.

$$\begin{aligned} &Q_i = a\frac{S_i - S_{i\min}}{S_{i\max} - S_{i\min}} + (1-a)\frac{R_i - R_{i\min}}{R_{i\max} - R_{i\min}}\ ) \\ &i = 1, 2, \cdots, n_o \end{aligned} \tag{B.5}$$

Step 4: Sorting the alternatives

Sort them in descending order according to Q_i.